Proceedings of the 1999 IEEE/RSJ
International Conference on
Intelligent Robots and Systems

# Characteristics of Optimal Solutions in Resolving Manipulator Redundancy under Inequality Constraints

Ki-Cheol Park*, Pyung-Hun Chang*, and Seung-Ho Kim**

Department of Mechanical Engineering
Korea Advanced Institute of Science and Technology
373-1 Gusong-dong, Yusong-gu, Taejon, Korea
E-mail: phchang@mecha.kaist.ac.kr

Department of Advanced Robotics Development
Korea Atomic Energy Research Institute
150 Deokjin-dong, Yusong-gu, Taejon, Korea

## Abstract

*This paper presents our finding of a critical point that has not been reported thus far in the inverse kinematics of redundant manipulators under inequality constraints. The critical point, named algorithmic barrier, was first encountered in the form of peculiar phenomena in our experiment of 8-DOF robot, which we believe to have the significance in the order of so-called algorithmic singularity. In addition, this paper deals with the characteristics of optimal solutions (COS) in resolving manipulator redundancy under inequality constraints.*

*In order to analyze the COS, analytic functions of sufficient conditions and critical point conditions are derived. As a result, we find that COS is drastically affected by the introduction of inequality constraints. That is, COS under no inequality constraints is known to change only at algorithmic singularity, while COS under inequality constraints turns out to change at semi-singularity and algorithmic barrier as well as algorithmic singularity.*

*We prove the existence the critical points and present their analytical properties by using a planar 3-DOF manipulator.*

## 1. Introduction

This paper presents our finding of *a critical point* that has not been reported thus far in the inverse kinematics of redundant manipulators under inequality constraints. The critical point was first encountered in the form of peculiar phenomena in our experiment of 8-DOF robot, KAEROT [1,2]. Through subsequent analysis, we have concluded that this point has the significance in the order of so-called *algorithmic singularity* [3]. Provided below are the background and context associated with the critical point.

It is well known that various positive attributes of a redundant manipulator result from the self-motion capability provided by its kinematic redundancy. According to the self-motion topologies, configuration space (C-space) and work space (W-space) of a manipulator are divided into several regions by critical manifolds of kinematic singularity [4]. The kinematic map resulting from such divisions gives valuable information for global path planning.

The kinematic map, however, changes drastically and so does the global behavior of a redundant manipulator in the presence of *physical limits*, such as joint angle limits, obstacles, and self-collision [5]. More specifically, *semi-singularity* resulting from the physical limits causes a re-structuring of global kinematic map [6].

While the two maps above are invaluable to understand the solution characteristics of inverse kinematics for redundant manipulators, they do not take into account the performance optimization or the use of additional constraints. Remember that in many cases the very rationale of the redundancy is to provide the capability to optimize and/or use additional constraints. Then you may be able to understand the significance of the following question: *What are the characteristics of optimal solutions (COS) under the physical limits?*

The answer to the question forms the core of our paper and leads to the finding of the aforementioned critical point named as *algorithmic barrier* (AB). In addition, on the basis of our newly obtained understanding on the COS, the extended Jacobian method (EJM) [3,7] can be extended to redundancy resolution under inequality constraints with all its advantages and without its shortcomings and critical points. By its advantages, we mean the ability to exactly optimize a performance measure and trace a cyclic joint configuration space path [8-10]. By its shortcomings, the algorithmic singularity and the wrong direction of optimization [8-10].

This paper is organized as follows. Section 2 presents inequality constrained optimality constraints and extended MCL, based on the necessary conditions. Then, COS under inequality constraints are analyzed along with numerical examples by using analytic functions of sufficient conditions and critical points. Finally, Section 3 draws conclusions.

## 2. Characteristics of Optimal Solutions under Inequality Constraints

### 2.1 Problem Statements

In general, the forward kinematic function of a manipulator is given as follows:

$$f(\theta) = x, \tag{1}$$

where $x$ denotes an $m$-dimensional vector representing the location of an end effector, $\theta$ an $n$-dimensional vector representing joint angle variables, and $f(\cdot)$ a vector consisting of $m$ scalar functions. For a redundant manipulator, $r = n - m$ is greater than zero and is termed the degree of redundancy (DOR). Given the forward kinematic function, its inverse kinematics can be described as the following set:

$$M(\theta) = \{\theta : f(\theta) = x\}, \tag{2}$$

which constitutes called the self-motion manifold (SMM) [1] representing all inverse maps of the workspace position $x$.

Physical limits, such as joint angle limits and obstacles, to be avoided may be naturally represented by inequality constraints

0-7803-5184-3/99/$10.00 © 1999 IEEE

as follows:

$$G_i(\boldsymbol{\theta}) \le 0 \quad (i = 1,\ldots,p), \tag{3}$$

where $G_i = 0$ corresponds to the safe boundary of a kinematic constraint, and $G_i < 0$ the permissible region outside of that boundary. Additional subtasks have been included with the type of a performance measure, $H(\boldsymbol{\theta}) \in \Re^1$, to be optimized.

Therefore, several researchers [2,13,14] have formulated the manipulator redundancy resolution problem with multiple subtasks into the following local constrained optimization problem with inequality constraints [11]:

$$\begin{aligned} &\text{maximize (or minimize) } H(\boldsymbol{\theta}) \\ &\text{subject to } \boldsymbol{f}(\boldsymbol{\theta}) = \boldsymbol{x} \text{ and } \boldsymbol{g}(\boldsymbol{\theta}) \le 0, \end{aligned} \tag{4}$$

where $\boldsymbol{g}(\boldsymbol{\theta}) = \left[G_1(\boldsymbol{\theta}) \quad G_2(\boldsymbol{\theta}) \quad \cdots \quad G_p(\boldsymbol{\theta})\right]^T$.

In order to solve this problem (4), the necessary and sufficient conditions are required. To this end, a Lagrange function $L$ can be defined as follows:

$$L(\boldsymbol{\theta},\boldsymbol{\lambda},\boldsymbol{\mu}) = H(\boldsymbol{\theta}) + \boldsymbol{\lambda}^T(\boldsymbol{f}(\boldsymbol{\theta}) - \boldsymbol{x}) + \boldsymbol{\mu}^T\boldsymbol{g}(\boldsymbol{\theta}) \tag{5}$$

with

$$\boldsymbol{\mu}^T\boldsymbol{g}(\boldsymbol{\theta}^*) = 0, \tag{6}$$

where $L$ is rendered to a dimensionless quantity; to this end, $\boldsymbol{\lambda} \in \Re^m$ and $\boldsymbol{\mu} \in \Re^p$ are assigned proper dimensions, respectively. The first-order derivatives of the Lagrange function leads to

$$\left(\frac{\partial L}{\partial \boldsymbol{\theta}}\right)^T\Bigg|_{\boldsymbol{\theta}=\boldsymbol{\theta}^*} = \boldsymbol{f}(\boldsymbol{\theta}^*) - \boldsymbol{x} = \boldsymbol{0}, \tag{7}$$

$$\left(\frac{\partial L}{\partial \boldsymbol{\lambda}}\right)^T\Bigg|_{\boldsymbol{\theta}=\boldsymbol{\theta}^*} = \boldsymbol{h}(\boldsymbol{\theta}^*) + \boldsymbol{J}(\boldsymbol{\theta}^*)^T\boldsymbol{\lambda} + \nabla\boldsymbol{g}(\boldsymbol{\theta}^*)^T\boldsymbol{\mu} = \boldsymbol{0}, \tag{8}$$

where $\boldsymbol{h} \equiv (\nabla H(\boldsymbol{\theta}))^T$, $\boldsymbol{J} = \nabla\boldsymbol{f}(\boldsymbol{\theta}) \in \Re^{m\times n}$ and $\nabla \equiv \partial/\partial\boldsymbol{\theta}$.

The necessary conditions of the constrained maximization (minimization) under inequality constraints are already given by the Kuhn-Tucker conditions [15], which consists of (6), (8), and the sign requirements of Lagrange multipliers, $\boldsymbol{\mu} \le (\ge)\boldsymbol{0}$, along with the active set of $A = \{i \mid G_i(\boldsymbol{\theta}) = 0, \boldsymbol{\mu} \le (\ge)\boldsymbol{0}\}$. In [15], one can find it in more detail and also find the corresponding sufficient conditions.

In this paper, however, we redefine the active set as follows:

$$A = \{i \mid G_i(\boldsymbol{\theta}) = 0\} \tag{9}$$

Note that this active set modified in this paper has no sign requirement of Lagrange multipliers and thus is different from the original active set in [15]. Without the sign requirement, our approach presents a wider set of necessary conditions irrespective of the direction of optimization (maximization or minimization). Furthermore, conditions for the direction of optimization exist only in the sufficient conditions proposed in this paper. This reorganization of the necessary and sufficient conditions is much more helpful for the analysis of the COS, which will be turned out later in this section. Then, the next two subsections will deal with deriving the new necessary and sufficient conditions, respectively.

## 2.2 Inequality Constrained Optimality Constraints and Extended Measure Constraint Locus

First of all, let us define a new index set given by

$$S = \{i \mid G(\boldsymbol{\theta}) = 0, \mu_i = 0\}, \tag{10}$$

which is called the switching set in this paper since a switching of an inequality constraint from active state to inactive one or vice versa occurs when the switching set exists. Subtracting the switching set from the active set lead to another set given by

$$\Phi = A - S = \{i \mid G_i(\boldsymbol{\theta}) = 0, \quad \mu_i \ne 0\}. \tag{11}$$

In this paper, this is called the effective set, which is needed to derive the necessary conditions of this subsection and the subsequent sufficient conditions in a consistent way. The number of indices in effective set is denoted by $\phi$, with $0 \le \phi \le r$. Let us define $\boldsymbol{g}_\phi\ (\in \Re^\phi)$ as the vector with $G_i\ (i \in \Phi)$ as an element and $\boldsymbol{\mu}_\phi$ as the corresponding Lagrange multiplier vector.

Since $\mu_j = 0\ (j \notin \Phi)$, equation (8) leads to

$$\boldsymbol{h}(\boldsymbol{\theta}^*) + \boldsymbol{J}(\boldsymbol{\theta}^*)^T\boldsymbol{\lambda} + \nabla\boldsymbol{g}_\phi(\boldsymbol{\theta}^*)^T\boldsymbol{\mu}_\phi = \boldsymbol{0}. \tag{12}$$

Meanwhile, Chang[7] proposed a full-rank $r\times n$ matrix $\boldsymbol{Z}$ representing the null space matrix of the Jacobian $\boldsymbol{J}$ as follows:

$$\boldsymbol{Z} = \left[\boldsymbol{J}_r\mathrm{Adj}(\boldsymbol{J}_m) \ \vdots\ -\det(\boldsymbol{J}_m)\boldsymbol{I}_r\right] \in \Re^{r\times n} \tag{13}$$

where $\boldsymbol{J} = \left[\boldsymbol{J}_m^T \ \vdots\ \boldsymbol{J}_r^T\right]$. Premultiplying both sides of (12) with $\boldsymbol{Z}$ leads to

$$\boldsymbol{Z}\boldsymbol{h}(\boldsymbol{\theta}) + \boldsymbol{Z}\nabla\boldsymbol{g}_\phi(\boldsymbol{\theta})^T\boldsymbol{\mu}_\phi = \boldsymbol{0} \tag{14}$$

since $\boldsymbol{Z}\boldsymbol{J}^T = \boldsymbol{0}$. If $\Phi = \{\}$, then (14) can be reduced to the following $r$ optimality constraints:

$$\boldsymbol{Z}\boldsymbol{h}(\boldsymbol{\theta}^*) = \boldsymbol{0} \quad \in \Re^r, \tag{15}$$

which are exactly the same as those of the EJM [6]. Because of the effective set, however, (14) still includes Lagrange multipliers $\boldsymbol{\mu}_\phi$. In order to get $\boldsymbol{\mu}_\phi$ out of (14) similar to (15), let us define

$$\boldsymbol{\lambda}_\phi \equiv \begin{bmatrix}\boldsymbol{\lambda} \\ \boldsymbol{\mu}_\phi\end{bmatrix} \tag{16}$$

and

$$\boldsymbol{J}_\phi \equiv \begin{bmatrix}\boldsymbol{J} \\ \nabla\boldsymbol{g}_\phi\end{bmatrix}. \tag{17}$$

Substituting these two relations into equation (12) leads to

$$\boldsymbol{h} + \boldsymbol{J}_\phi^T\boldsymbol{\lambda}_\phi = \boldsymbol{0}. \tag{18}$$

Similar to $\boldsymbol{Z}$, we can derive $\boldsymbol{Z}_\phi \in \Re^{(r-\phi)\times n}$ representing the null space matrix of $\boldsymbol{J}_\phi$ with the relationship of $\boldsymbol{Z}_\phi\boldsymbol{J}_\phi^T = \boldsymbol{0}$. Then, by premultiplying both sides of (18) with $\boldsymbol{Z}_\phi$, we obtain

$$\boldsymbol{Z}_\phi\boldsymbol{h} = \boldsymbol{0} \quad \in \Re^{r-\phi}. \tag{19}$$

Finally, we have $r$ independent equations, called inequality-constrained optimality constraints (ICOC), as follows:

$$\begin{aligned} &\boldsymbol{g}_\phi(\boldsymbol{\theta}) = \boldsymbol{0} \quad \in \Re^\phi \\ &\boldsymbol{Z}_\phi\boldsymbol{h}(\boldsymbol{\theta}^*) = \boldsymbol{0} \quad \in \Re^{r-\phi} \end{aligned}, \tag{20}$$

which constitute the new necessary conditions of the constrained optimization problem under inequality constraints.

In order to effectively visualize in C-space a set of optimal solutions satisfying the necessary conditions (20) of constrained optimization under no inequality constraints, the measure constraint locus (MCL) [7] was proposed as the following set:

$$\Psi = \{\boldsymbol{\theta} : \boldsymbol{Z}\boldsymbol{h}(\boldsymbol{\theta}) = \boldsymbol{0}\}. \tag{21}$$

However, the MCL cannot be applied to inequality constrained optimization. Thus, we define a new MCL under inequality constraints, called the extended MCL (EMCL), as the set of configurations satisfying the ICOC such that

$$\Psi_e = \{\theta : g_\phi(\theta) = 0,\ Z_\phi h(\theta) = 0\}. \quad (22)$$

Since SMM and EMCL are homogeneous solutions and optimality constraints of a constrained optimization problem under inequality constraints, respectively, a set of inverse kinematic solutions can be uniquely determined by overlapping them in C-space. Further, EMCL can be classified into the following two types: one is EMCL on free space (EMCLFS) given by

$$\Psi_{fs} = \{\theta : Z_\phi h(\theta) = 0\}. \quad (23)$$

and the other is EMCL on physical limits (EMCLPL) given by

$$\Psi_{kc} = \{\theta : g_\phi(\theta) = 0\}. \quad (24)$$

Then, the switching set exists where the EMCLFS and EMCLPL meet each other.

## 2.3 Sufficient Conditions

Redundancy resolution methods using only necessary conditions often result in wrong direction of optimization. That is, even if maximization is needed, minimization may occur. Hence, a method is needed that serves as a discriminant to discern the right direction of optimization. In a redundancy resolution problem under no inequality constraints, the characteristic of an optimal solution (COS) means whether the solution is (local) maximum, minimum, or algorithmic singularity. In general, COS can be easily identified by sufficient conditions.

This idea can be extended to a redundancy resolution problem under inequality constraints. That is, an optimal solution satisfying the necessary conditions (20) may be (local) maximum, minimum, or else. In order to identify COS, in this section, we propose simple and analytical functions for sufficient conditions of redundancy resolution (or constrained optimization) with the following theorem.

**Theorem 1** (sufficient conditions of constrained maximization (minimization)): On a non-singular joint configuration $\theta^*$ satisfying (1), (3), and (20), $\theta^*$ is a local maximum (or minimum) point for the constrained optimization problem if $\mu_\phi(\theta^*)$ is negative (or positive) and if $C_\phi(\theta^*)$ is negative (or positive) definite such that

$$\mu_\phi(\theta^*) = -D\left(J_\phi W_d^{-1} J_\phi^T\right)^{-1} J_\phi W_d^{-1} h(\theta^*) \quad \in \Re^\phi, \quad (25)$$

$$C_\phi(\theta^*) = \nabla\left(Z_\phi h\right) Z_\phi^T(\theta^*) \quad \in \Re^{r-\phi}, \quad (26)$$

where $D = \left[0_{\phi\times m} \ \vdots \ I_{\phi\times\phi}\right] \in \Re^{\phi\times(m+\phi)}$ denotes a kind of selection matrix and $W_d$ the weight matrix for dimensional consistency.

**Proof :** proof is omitted by the page limit.

By using Theorem 1 of the sufficient conditions, EMCL can be further divided into max. EMCL and min. EMCL. Note that there exist critical points at which max. EMCL and min. EMCL meet each other, some of which are neither maximum nor minimum. Next subsection will analyze the critical points.

## 2.4 Critical Points

As one of redundancy resolution methods under no inequality constraints, the well-known extended Jacobian method (EJM) is known to have the problem of algorithmic singularity (AS) [8-10]. Furthermore, the invertible work space of EJM is limited by AS [8]. AS always occurs at a point on the MCL where SMM is tangent to MCL [8-10], as is illustrated in C-space in Fig. 1. Note that MCL under no inequality constraints is almost the same as EMCLFS under inequality constraints. In the left of Fig. 1, thin solid lines with $M_i$ $(i = 1,2,3)$ denote SMM, thick solid lines max. MCL, and thick dashed lines min. MCL. In Fig. 1, MCL meets $M_1$ at two points $P_a$ and $P_c$, while MCL is tangent to $M_2$ at $P_b$. Let us define $z = Z_\phi^T$ and $y = \left(\nabla Z_\phi h\right)^T$ at each point. Then, $C_\phi = y^T z$. As the result, we obtain $C_\phi < 0$ (max.) at $P_a$, $C_\phi > 0$ (min.) at $P_c$, and $C_\phi = 0$ (singular) at $P_b$, which is summarized in Table 1. This feature can also be easily understood through the plots of performance measure on $M_i$ $(i = 1,2,3)$ in the right of Fig. 1. That is, AS always exists at the border of max. MCL and min. MCL. Therefore, when the EJM is applied, the characteristic of an initial equilibrium solution (max. or min.) is invariant before AS, if any [10]. Consequently, COS changes *only* at AS along MCL in constrained optimization under no inequality constraints. Thus, it is easy to believe that this still holds in constrained optimization under inequality constraints.

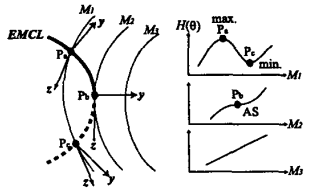


$M_i$ $(i = 1,2,3)$: SMM, $z = Z_\phi^T$, $y = \left(\nabla Z_\phi h\right)^T$

Fig. 1: Algorithmic singularity

Table 1: COS at the three points in Fig.1 through Fig. 3

| | $P_a$ | $P_b$ (critical point) | $P_c$ |
|---|---|---|---|
| Fig. 1 | $C_\phi < 0$ | $C_\phi = 0$ (AS) | $C_\phi > 0$ |
| (a) of Fig. 2 | $\mu_k > 0$ | $\mu_k = \pm\infty$ (SS1) | $\mu_k < 0$ |
| (b) of Fig. 2 | $\mu_k < 0$ | $\mu_k = \pm\infty$ (SS2) | $\mu_k > 0$ |
| (c) of Fig. 2 | $\mu_k > 0$ | $\mu_k$ sign-indefinite (SS3) | $\mu_k < 0$ |
| (a) of Fig. 3 | $\mu_k < 0$ | $\mu_k = 0$, $C_\phi > 0$ (AB1) | $\mu_k > 0$ |
| (b) of Fig. 3 | $\mu_k > 0$ | $\mu_k = 0$, $C_\phi < 0$ (AB2) | $\mu_k < 0$ |
| (c) of Fig. 3 | $\mu_k < 0$ | $\mu_k$ sign-indefinite (AB3) | $\mu_k > 0$ |

Note: $C_\phi < 0$ and $\mu_k < 0$ denote maximum state, while $C_\phi > 0$ and $\mu_k > 0$ minimum state.

In this paper, however, we found that inequality constraints drastically affect the COS. That is, COS changes at semi-singularity (SS) and algorithmic barrier (AB) as well as AS along EMCL. On the one hand, SS is a kinematic condition in which the end-effector is unable to generate velocity in a particular direction, while still capable of generating velocity in the opposite direction[5]. That is, SS is uni-directional, while kinematic singularity (KS) is bi-directional [6]. However, the effect of SS on the global behavior of redundant manipulators is

almost the same as that of KS. The fundamental property of SS is that it always occurs at a point on the boundary of physical limits where SMM is tangent to such a boundary [5,6], which is illustrated in Fig. 2. The shaded regions with $G_k > 0$ in Fig. 2 denotes the inside of obstacles. SS is originally divided into two cases: one is smooth tangency case (a) and (b); and the other is non-smooth tangency case (c). In this paper, we further divide the smooth tangency case into two types because SS of (a) is inescapable by self-motion, while SS of (b) is escapable. As the result, there exist three types of semi-singularity. Let us define $\nu = (\nabla G_k)^T$ at the three points. Then, we obtain $\mu_\phi = \mu_k = -\dfrac{z^T h}{z^T \nu}$. The COS at each point in each type of semi-singularity is also shown in Table 1. From the Fig. 2 and Table 1, it turns out that COS also changes at SS.

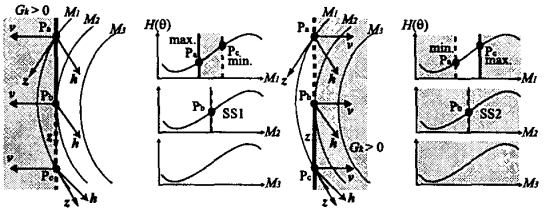


(a) Semi-singularity type-1 (b) Semi-singularity type-2

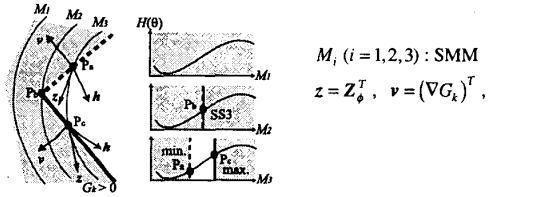


$M_i$ $(i = 1,2,3)$ : SMM

$z = Z_\phi^T$, $\nu = (\nabla G_k)^T$,

(c) Semi-singularity type-3

Fig. 2: Semi-singularities

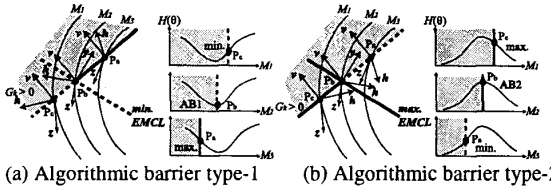


(a) Algorithmic barrier type-1 (b) Algorithmic barrier type-2

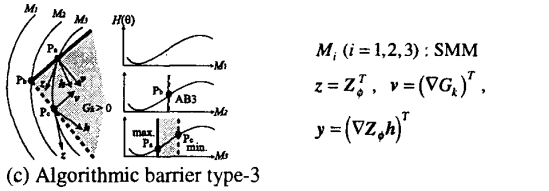


$M_i$ $(i = 1,2,3)$ : SMM

$z = Z_\phi^T$, $\nu = (\nabla G_k)^T$,

$y = (\nabla Z_\phi h)^T$

(c) Algorithmic barrier type-3

Fig. 3: Algorithmic barriers

On the other hand, AB as well as AS does not affect the global behavior of redundant manipulators, different from KS and SS. That is, AB and AS occur only when we use optimization of a performance measure additionally. Fig. 3 and Table 1 illustrates the three types of AB and why COS changes at each AB. Note that AB type-1 is called AB against maximization, AB type-2 AB against minimization, and AB type-3 against both of them. In other words, AB type-1 is not AB for minimization and AB type-2 is not AB for maximization since there exists a way on MCLFS along which COS does not change. It is noteworthy that the condition of AB3 ($\mu_k$ is sign-indefinite) is the same as that of SS3. The only difference between the two depends on whether the point is escapable by self-motion or not.

In the end, Table 2 summarizes when each critical point occurs in general. Note that thanks to the reorganization along with the new active set and the effective set, the sufficient conditions and the critical point conditions can be derived with the same function in a consistent way.

Table 2: Conditions of critical points

| Type | Conditions of critical points |
|---|---|
| AS | $C_\phi(\theta^*)$ is singular |
| SS1 | $\mu_k(\theta^*) = \pm\infty$ and inescapable by self-motion |
| SS2 | $\mu_k(\theta^*) = \pm\infty$ and escapable by self-motion |
| SS3 | $\mu_k(\theta^*) (\neq 0)$ is sign-indefinite and inescapable by self-motion |
| AB1 | $\mu_k(\theta^*) = 0$ and $C_\phi(\theta^*)$ is positive definite |
| AB2 | $\mu_k(\theta^*) = 0$ and $C_\phi(\theta^*)$ is negative definite |
| AB3 | $\mu_k(\theta^*) (\neq 0)$ is sign-indefinite and escapable by self-motion |

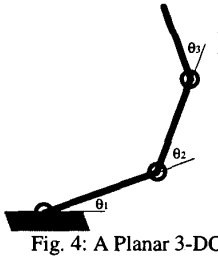


$l_1 = 3.0$

$l_2 = 2.5$

$l_3 = 2.0$ units

Fig. 4: A Planar 3-DOF manipulator

## 2.5 Examples

By using examples, in this subsection, we will prove that COS changes at AS, SS, and AB along EMCL and will analyze the global properties of COS and EMCL. Consider a planar 3-DOF manipulator with link lengths of $l_1 = 3.0$, $l_2 = 2.5$, and $l_3 = 2.0$ units as shown in Fig. 4.

As for a performance measure to be maximized, we choose the manipulability measure [12], which have been widely used for a subtask of dexterity improvement and singularity avoidance and which is given by

$$H(\theta) = \sqrt{\det(JJ^T)}. \quad (27)$$

As for physical limits, the following three situations are considered in turn:

a) under no physical limits,

b) under angle limits of the second joint ($60^o \le \theta_2 \le 265^o$),

c) under angle limits of the second and third joints ($60^o \le \theta_2 \le 265^o$ and $-120^o \le \theta_3 \le 170^o$).

### 2.5.1 under no physical limits

Irrespective of the measure, the simulated manipulator has 3 (escapable) KS's, that are shown as squares in Fig. 5(a). Their corresponding SMM, shown as thin solid lines in Fig. 5(a), globally divides C-space into 4 C-bundles, respectively, in light of self-motion topology[1].

Meanwhile, if we consider optimization of the manipulability measure in this case, MCL (or EMCLFS) can also be shown in Fig. 5(a), where thick solid and dashed lines represent max. MCL and min. MCL, respectively. As for max. MCL satisfying both necessary and sufficient conditions, there are 6 groups denoted by A1 through C2. At the ends of max. MCL's, we can easily identify 10 AS's, shown as triangles in Fig. 5(a), as the points where SMM is tangent to MCL and where max. MCL meets min. MCL.

Note that max. MCL also meets min. MCL at KS with $\theta_2 = \theta_3 = 0^o$. However, this kind of KS is excluded in this analysis since it is on the boundary of the workspace. Consequently, COS changes only at AS in constrained optimization under no inequality constraints.

### 2.5.2 under a joint angle limit (1 JAL)

Fig. 5(b) shows that due to a joint angle limit, the manipulator has 2 KS's, 2 SS1's and 2 SS2's, which divides C-space into 6 C-bundles. As denoted by circles in Fig. 6, SS1 and SS2 occur at a point on the boundary of the joint angle limit, where SMM is tangent to such a boundary.

Similarly, if we consider optimization of the measure in this case, along with EMCL, 8 AS's, 4 AB1's and 4 AB2's appear additionally at which COS changes. As for max. EMCL, there are 8 groups denoted by A1 through E, with SS, AS and AB at their both ends. To sum up, it is verified that COS under inequality constraints is different from those under no inequality constraints and changes at SS1, SS2, AB1, and AB2 as well as AS.

### 2.5.3 under 2 joint angle limits (2 JAL's)

In this case, there newly appears 1 SS3, shown as a filled circle at $\theta_2 = 60^o$ and $\theta_3 = 170^o$ in Fig. 5(c). As the result, the manipulator has 1 KS, 2 SS1's, 3 SS2's and 1 SS3, which divide C-space into 7 C-bundles different in self-motion topology.

Similarly, if we consider optimization of the measure in this case, along with EMCL, 7 AS's, 7 AB1's and 3 AB2's appear additionally at which COS changes.[2] As for max. EMCL, there appear 10 groups denoted by A1 through H, with SS, AS and AB at their both ends.

Through the examples, it is finally verified that COS changes at AS, SS and AB, while self-motion topology changes at KS and SS, and that critical points exist at the ends of EMCL groups. Thus, redundancy resolution problem can be transformed into selecting and following an appropriate EMCL group.

[1] The physical motion of the links in a self-motion are similar only in a C-bundle, but changes when crossing a singularity manifold [1].

[2] AB3 does not appear in these three examples, but it is easy to show that COS also changes at AB3.

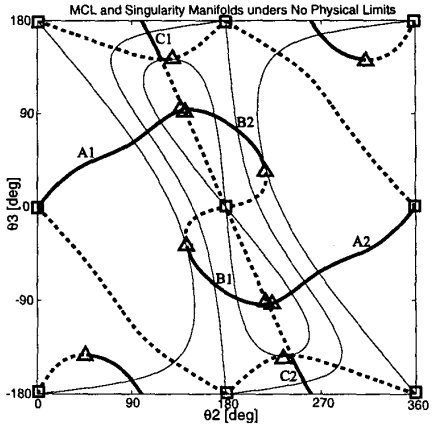


(a) under no inequality constraints

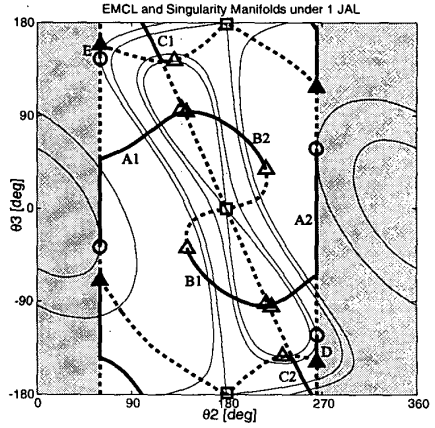


(b) under $60^o \le \theta_2 \le 265^o$

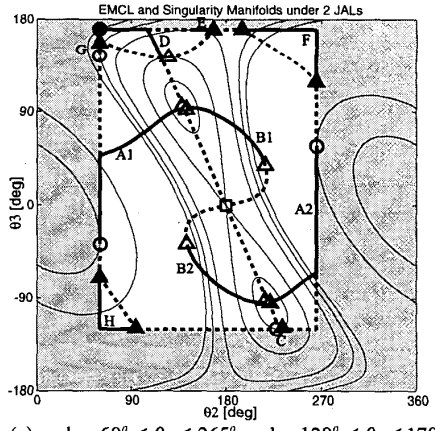


(c) under $60^o \le \theta_2 \le 265^o$ and $-120^o \le \theta_3 \le 170^o$

——— (singularity manifold)

▬▬ (maximum locus) ▪▪▪▪ (minimum locus)

□ (KS) ○ (SS1, SS2) ● (SS3) △ (AS) ▲ (AB1)

Fig. 5: EMCL and singularity manifolds

Table 3: Existence of Critical Points

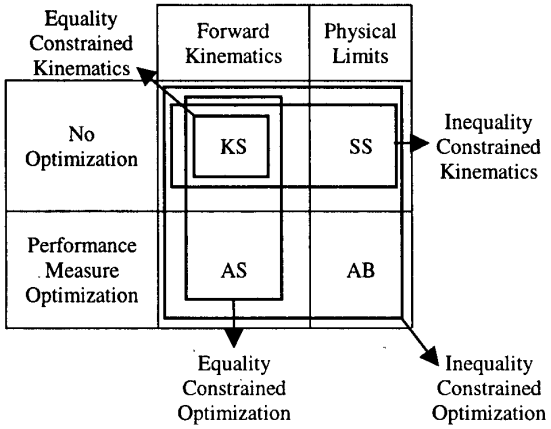


Meanwhile, it is also noteworthy that different kinds of critical points appear according to situations. More specifically, as shown in Table 3, when only the forward kinematic function is considered (in case of equality constrained kinematics), there appears only KS. When an optimization problem is added to this situation (in case of equality constrained optimization), AS appears additionally. Meanwhile, when there exist physical limits (in case of inequality constrained kinematics) without any measure, SS appears with KS. In case of inequality constrained optimization, finally, all critical points including AB show up.

## 3. Conclusions

The characteristics of optimal solutions (COS) in resolving manipulator redundancy under inequality constraints were first analyzed in this paper, which are greatly different from those under no inequality constraints. To visualize COS, we proposed the extended measure constraint locus (EMCL), which is the set of configurations satisfying the necessary conditions for constrained optimization under inequality constraints.

As the results, in this paper, it turned out that based on the COS, optimal solutions are divided into local max., local min., algorithmic singularity (AS), semi-singularity (SS) and algorithmic barrier (AB). In addition, COS under no inequality constraints is known to change at AS, while COS under inequality constraints turned out to change at critical points such as SS and AB as well as AS.

The analytic functions of sufficient conditions and critical points are crucial to this analysis. With the help of these functions, we do not need to depend on the graphical analysis of EMCL.

By using the necessary conditions and the analytic functions for COS, a new redundancy resolution method[3] can be made, which is an exact extension of the EJM to redundancy resolution under inequality constraints and which can exactly perform the main task starting from the best initial configuration while avoiding physical limits and exactly optimizing a performance measure with cyclic behavior.

[3] The section for introducing the new redundancy resolution method is omitted in this paper because of the page limit.


## Acknowledgment

This project has been carried out under the nuclear R&D program by the Ministry of Science and Technology in Korea.


## References


[1] *The Development of Advanced Robotics for the Nuclear Industry - The Development of Robotic System for the Nuclear Power Plants*, Report No. KAERI/RR-1508, Korea, 1994.

[2] Ki C. Park, P.H. Chang, and J.K. Salisbury, "A Unified Approach for Local Resolution of Kinematic Redundancy with Inequality Constraints and Its Application to Nuclear Power Plant," in *Proc. IEEE ICRA*, pp.766-773, 1997.

[3] J. Bailieul, "Avoiding Obstacles and Resolving Kinematic Redundancy," *Proc. IEEE Int. Conf. Robotics and Automation*, pp. 1698-1704, 1986.

[4] J.W. Burdick, "On the Inverse Kinematics of Redundant Manipulators: Characterizations of the Self-Motion Manifold," in *Proc. IEEE ICRA*, pp. 264-270, 1989.

[5] C.L. Luck and S. Lee, "Self-Motion Topology for Redundant Manipulators with Joint Limits," in *Proc. IEEE ICRA*, pp.626-631, 1993.

[6] C.L. Luck and S. Lee, "Redundant Manipulators under Kinematic Constraints: A Topology-Based Kinematic Map Generation and Discretization," in *Proc. IEEE ICRA*, pp.1-6, 1995.

[7] P.H. Chang, "A Closed-Form Solution for Inverse Kinematics of Robot Manipulators with Redundancy," *IEEE J. Robotics and Automation*, Vol. RA-3, No. 5, pp. 393-403, 1987.

[8] B.W. Choi, J.H. Won, and M.J. Chung, "Manipulability Constraint Locus for a Redundant Manipulator," in *Proc. IEEE/RSJ IROS*, pp.167-172, 1991.

[9] D.K. Cho, B.W. Choi, and M.J. Chung, "Optimal Conditions for Inverse Kinematics of a Robot manipulator with redundancy," Robotica, vol.13, pp.95-101, 1995.

[10] J. Park, W.-K. Chung, and Y. Youm, "Characteristics of Optimal Solutions in Kinematic Resolutions of Redundancy," *IEEE Trans. Robotics Automat.*, vol.12, no.3, pp.471-478, 1996.

[11] D.G. Luenberger, *Linear and Nonlinear Programming*, 2nd ed. Addison-Wesley Publishing Company, 1984.

[12] T. Yoshikawa, "Manipulability of Robotic Mechanism," *Int. J. Robotics Res.* vol..4, no.2, pp.3-9, 1985

[13] H. Seraji, "Configuration Control of Redundant Manipulators: Theory and Implementation," IEEE Trams. Robotics and Automation, vol.5, no.4, pp.472-490, 1989.

[14] Y.W. Sung, D.K. Cho, and M.J. Chung, "A Constrained Optimization Approach to Resolving Manipulator Redundancy," J. Robotic Systems, vol.13, no.5, pp.275-288, 1996.